Molecular Dynamics

DOI: 10.1002/ange.200602807

How Flexible Are Poly(*para*-phenyleneethynylene)s?**

*Adelheid Godt, Miriam Schulte, Herbert Zimmermann, and Gunnar Jeschke**

Molecules are often seen as geometrically well-defined building blocks for nanosized objects. Prominent examples are oligo(*para*-phenyleneethynylene)s (oligoPPEs), which are viewed as molecular rods despite their distinct flexibility.[1] Quantitative knowledge about intrinsic flexibility is required for designing functional nanostructures as well as for understanding the mechanical and dynamic properties of molecules. This knowledge can, in principle, be gained from the end-to-end-distance distribution.[2] Information about distance dis-

[*] Prof. Dr. G. Jeschke[+]
Max-Planck-Institut für Polymerforschung
Postfach 3148, 55131 Mainz (Germany)
Fax: (+49) 6131-379-100
E-mail: gunnar.jeschke@uni-konstanz.de
Prof. Dr. A. Godt, M. Schulte
Universität Bielefeld, Fakultät für Chemie
Universitätsstrasse 25, 33615 Bielefeld (Germany)
Dr. H. Zimmermann
Max-Planck-Institut für medizinische Forschung
Jahnstrasse 29, 69120 Heidelberg (Germany)
[+] Current address:
Universität Konstanz, Fachbereich Chemie
Universitätsstrasse 10, 78457 Konstanz (Germany)

[**] This work was supported by the Deutsche Forschungsgemeinschaft. The authors thank M. K. Bowman for an insightful discussion on orientation selection and C. Bauer for technical assistance.

Supporting information for this article is available on the WWW under http://www.angewandte.org or from the author.

tributions in the nanometer range has recently become accessible by techniques that measure the dipole–dipole interaction between two spin labels.[3] Such measurements can be performed with high precision by pulsed electron–electron double resonance (ELDOR) methods.[4] Recently, this technique was used to characterize the flexibility of bispeptide nanostructures on the basis of the standard deviation of the label-to-label distance distribution.[5] Quantification in terms of a reliable persistence length does, however, require elimination of the contribution of the labels to the distance distribution. Herein we show that such an elimination is possible and that the end-to-end distance distribution $P(r_{EE})$ of oligoPPE backbones can be obtained from pulsed ELDOR data to provide an estimate of the persistence length of polyPPEs.

We concentrate on oligomers because their comparatively small size allows their step-by-step synthesis and therefore a better control of the molecular structure than is possible for polymers. Side products that result from oxidative alkyne dimerization and carbometalation during the Sonogashira–Hagihara coupling, the key reaction for the synthesis of these oligomers and polymers, can be separated from the product.[6] Additionally, the limited purity of the monomers speaks in favor of oligomers: If one assumes that the monomers 1,4-diiodobenzene and 1,4-diethynylbenzene are contaminated with only 0.1% of the constitutional 1,3-isomers, nearly all chains of a polymer batch with a polymerization degree of 1000 contain one *meta* linkage. This polymerization degree is typical for samples used in light-scattering experiments,[7] which is the standard technique for determining the persistence length. *Meta* linkages will reduce the radius of gyration and hence the apparent persistence length.[8] In contrast, only one out of 100 molecules has this defect in the case of a decamer.

Pulsed electron paramagnetic resonance (EPR) techniques[9] are well suited for characterizing structures of 2–8 nm in length.[4,10] At these distances backbone flexibility strongly influences the shape of $P(r_{EE})$ for persistence lengths of the order of 15 nm. Such a persistence length is expected for polyPPEs on the basis of an earlier extensive light-scattering study.[7] The principal limitation of EPR techniques is their requirement for spin labeling, so that the label-to-label-distance distribution $P(r_{LL})$ rather than $P(r_{EE})$ is measured (Scheme 1). The contribution of the labels to $P(r_{LL})$ can be eliminated and thus $P(r_{EE})$ obtained by synthesizing[11] and measuring a series of compounds with the same labeling pattern and backbone structure but different backbone length.

Elimination of the label contribution requires a model for the distribution of conformations of both the label and the backbone. It is necessary to model the backbone, as $P(r_{EE})$ can only be obtained from $P(r_{LL})$ when the distribution of the relative orientations of the backbone ends is also known. We model the backbone as a sequence of jointed stiff segments. As segments we define the phenylene ring, the bond between a phenylene and an ethynylene unit, the triple bond, and the bond between two ethynylene units. The relative segment lengths r_j are taken from the MMFF force field.[12] The angle θ_j at the joint between two segments (Figure 1) is determined by a harmonic bending potential. The bending potential for joints at a phenylene segment is half as large as that for all other joints within the backbone. All torsion angles φ_j are equally likely; that is, the chain rotates freely at its joints, which agrees well with our molecular dynamics (MD) simulations of oligoPPEs. A general stretch factor s for the segment length and the bending potential F_B for the non-phenylene joints are the two fit parameters of the backbone model. The labels are modeled as additional stiff segments of

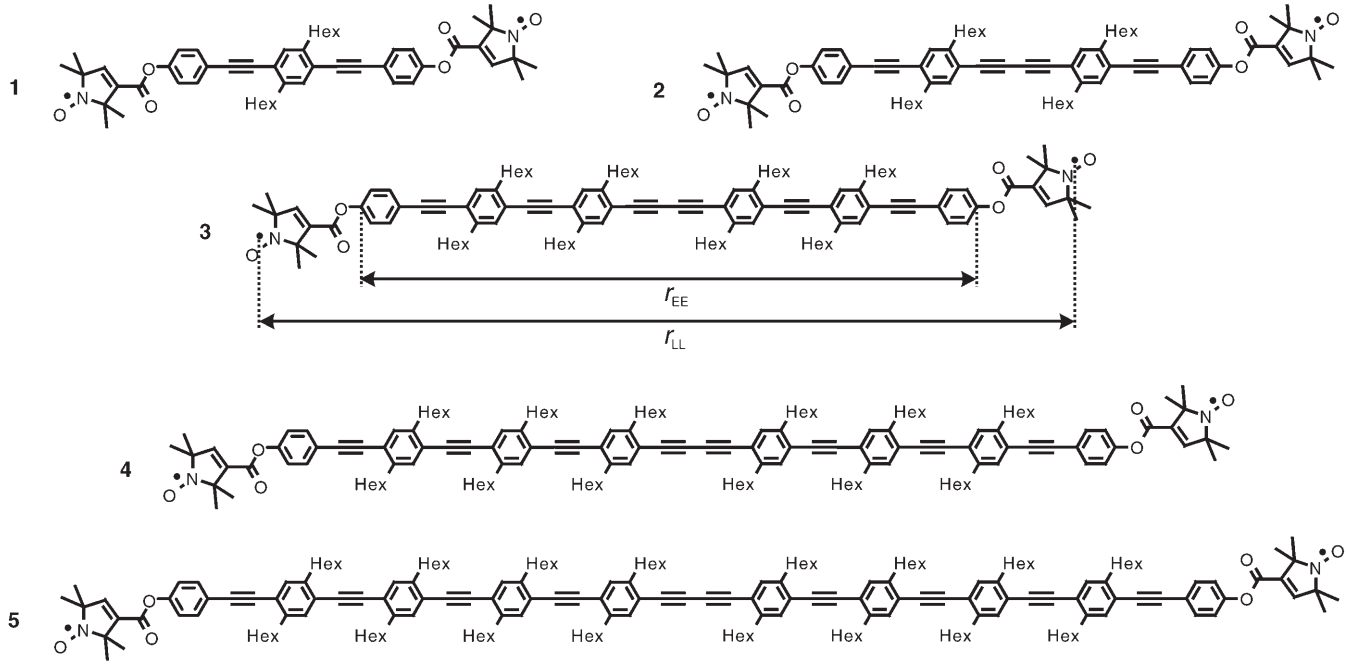

Scheme 1. Structures of the biradicals used and definition of the label-to-label distance r_{LL} and backbone end-to-end distance r_{EE}.

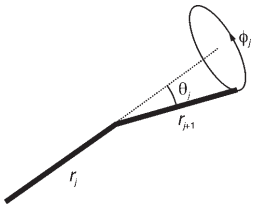

Figure 1. Coarse-grained model for the conformation of the PPE backbone consisting of consecutive segments j and $j+1$ with lengths r_j and r_{j+1}. The segment $j+1$ rotates freely about the dotted axis. For angle θ_j, a normal distribution with a mean value of zero is assumed. The same model is used for the end labels.

length l jointed to the first and last phenylene unit of the backbone with an effective bending potential B. The distribution of label conformations is thus accounted for by two additional fit parameters l and B.

To test whether this model properly separates the label and backbone contribution to $P(r_{LL})$, we applied it to results of MD simulations for **2**–**4** that were obtained with the PCFF force field. The $P(r_{LL})$ and the true $P(r_{EE})$ were extracted from the MD trajectories. The model was fitted to the $P(r_{LL})$ of the three compounds simultaneously. Fit parameters are given in Table 1, and the apparent $P(r_{EE})$ for the ensemble of

Table 1: Best-fit values of the stretch factor s, backbone bending potential F_B, label length l, and effective label bending potential B in the conformational model for oligoPPEs.

Fitted data	s	F_B [k_BT]	l [nm]	B [k_BT]
MD	0.993	38.4	0.650	2.023
DEER	0.991	20.0	0.646	2.019

modeled conformations is compared to the true $P(r_{EE})$ in Figure 2 for each compound. The good agreement justifies the use of the same model for extracting $P(r_{EE})$ from pulsed ELDOR data.

In earlier four-pulse double electron–electron resonance (DEER) measurements on compounds **1** and **3**[3a,4d] we noticed that effects of orientation selection[13] were apparent

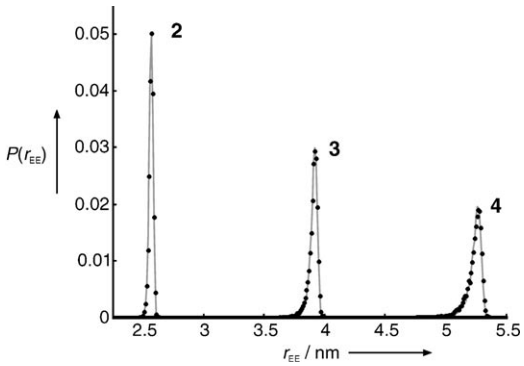

Figure 2. End-to-end distance distributions $P(r_{EE})$ from MD simulations of compounds **2**–**4**. Black dots correspond to the true $P(r_{EE})$ extracted directly from the MD trajectories and gray solid lines to the apparent $P(r_{EE})$ obtained by model-based elimination of the label contribution from the label-to-label distance distribution $P(r_{LL})$.

in dipolar spectra and caused a systematic deviation of the experimental time-domain data from fits during the first dipolar oscillation. Such a systematic deviation might compromise the fitting of the conformational model, in particular for the longer oligomers **4** and **5**, for which only few oscillations can be observed. We therefore introduce orientation averaging by varying the magnetic field so that the observer position is swept between the low-field maximum of the nitroxide spectrum and the global maximum in 23 steps of 0.1 mT. The difference between pump and observer frequency is kept constant at 65 MHz. This procedure virtually eliminates orientation selection and systematic deviations of the fit (Figure 3).

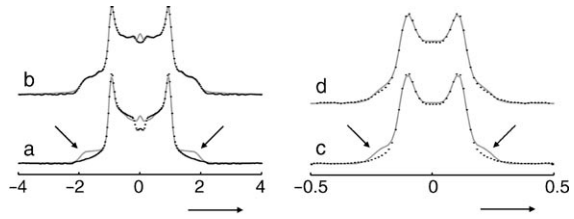

Figure 3. Improved orientation averaging in dipolar spectra obtained by the four-pulse DEER experiment on **2** (a,b) and **5** (c,d). Black dots correspond to experimental data and gray solid lines to simulations for which an ideal powder average is assumed. a,c) Fixed observer and pump positions. Arrows mark deviations due to the suppression of orientations along the spin–spin vector. b,d) Orientation averaging.

To obtain the end-to-end distance distributions $P(r_{EE})$ from the orientation-averaged DEER data, we simultaneously fitted the conformational model to the experimental form factors $F(t)$ of all five compounds. The $F(t)$ values were obtained from the primary experimental data by correcting for the intermolecular background. In our approach the label-to-label distance distributions $P(r_{LL})$ computed with the conformational model are converted into simulated form factors by straightforward matrix multiplication. The other possible approach of converting the experimental $F(t)$ values into distance distributions $P(r_{LL})$ would require the solution of an ill-posed inverse problem and thus compromise the reliability of the fit.[3]

Our conformational model with four variable parameters fits the experimental form factors of all five compounds quite closely (Figure 4). Furthermore, the label length l and

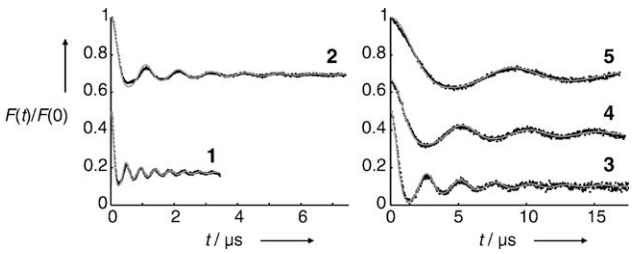

Figure 4. Global fit of the conformational model for oligoPPEs to experimental form factors $F(t)$. Black dots represent experimental data, gray solid lines simulations corresponding to the parameters in Table 1.

effective label bending potential B agree nicely with the results for the MD data (Table 1), which suggests that an MD simulation in vacuo describes the conformational distribution of the nitroxide end labels quite well. Likewise, good agreement between the MD and DEER data was found for the stretch factor s for the contour length of the backbone. The stretch factor s is close to the ideal value of unity.

In contrast, the bending potential F_B of the backbone joints is smaller for the DEER than for the MD data by almost a factor of two (Table 1). This deviation by far exceeds experimental error. We therefore conclude that the backbone of oligoPPEs is significantly more flexible than suggested by our MD simulations (Figure 2). This greater flexibility is in line with calculation-based predictions for related semiflexible polymers.[14]

The experimental $P(r_{EE})$ results for all compounds are shown in Figure 5 together with a global fit by the Kratky–Porod wormlike-chain (WLC) model; an analytical expression[2] for $P(r_{EE})$ has been used. Within the limits of experimental precision our data agree with this model. The best-fit persistence length is 17.5 nm.

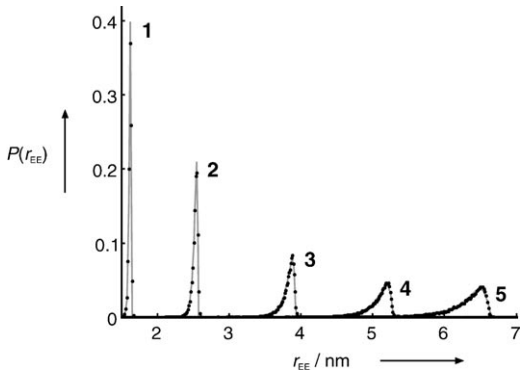

Figure 5. End-to-end distance distributions $P(r_{EE})$ for oligoPPE backbones. Black dots correspond to $P(r_{EE})$ extracted from DEER data, and gray solid lines show a global fit by the WLC model.

If we fit the WLC model to the individual $P(r_{EE})$ of the five compounds, we find persistence lengths of 14.3, 16.9, 18.2, 19.2, and 19.1 nm for **1**, **2**, **3**, **4**, and **5**, respectively. This trend is probably due to the fact that our conformational model, unlike the WLC model, allows for some variation in the contour length by bond-stretching vibrations. The longer the oligomer, the more backbone flexibility dominates the broadening of the distance distribution, so that the data for **4** and **5** are more reliable. Apparently, the persistence length approaches an asymptotic limit of about 19 nm for theses two oligomers. From the contour lengths obtained by the WLC fits we find that one *para*-phenyleneethynylene repeat unit increases the contour length by 0.688 nm.

Although the investigation is restricted to oligomers with a length of up to 8 nm, it provides the persistence length of polyPPE, because the persistence length is a property that depends only on the structure of the repeating units and not on the length of the molecule. Light-scattering experiments on polydisperse polyPPEs gave distinctly shorter persistence lengths of between 13.5 and 16 nm.[7] The difference between the two sets of results may be partially due to the different side groups.[15] It may also hint at the presence of constitutional defects, such as *meta* linkages. For validation, samples of polyPPEs of different origin formed by different synthetic routes[16] need to be investigated.

In summary, we have introduced a new approach for the experimental characterization of the flexibility of shape-persistent molecules. This approach is based on the synthesis of a series of oligomers, spin labeling, the measurement of spin-to-spin distance distributions, and the extraction of the end-to-end distance distribution of the backbone by modeling the conformational ensemble. As information on the residual flexibility of shape-persistent molecules is a key requirement for the rational design of well-defined nanostructures, this approach should find applications well beyond the determination of the persistence length of semiflexible polymers.

Experimental Section

Synthesis: Compounds **1**–**3** were synthesized as described previously.[11] Compounds **4** and **5** were synthesized analogously. Synthetic procedures and analytical data are given in the Supporting Information.

DEER measurements: Glassy frozen solutions of biradical (**1**, **2**: 1.5 mmol L^{-1}; **3**, **4**, **5**: 0.4 mmol L^{-1}) in perdeuterated *o*-terphenyl were analyzed by a variable-time four-pulse DEER experiment on a Bruker E580 spectrometer at a temperature of 50 K.[4b,c,d] Details are given in the Supporting Information.

Modeling: Molecular-dynamics simulations were run for a total time of 2 ns with the program package Cerius2 (v.3.8, Molecular Simulations, Inc.) by using the PCFF force field and a Nosé–Hoover thermostat to generate a canonical ensemble. Distance distributions $P(r_{LL})$ and $P(r_{EE})$ within our conformational model were computed by Monte Carlo simulations by using a home-written Matlab (The MathWorks, Inc., Natick, MA, USA) program. Details are given in the Supporting Information.

Received: July 14, 2006
Published online: October 18, 2006

Keywords: chain model · EPR spectroscopy · polymers · shape persistence · spin labeling

[1] See, for example: a) S. Rucareanu, O. Mongin, A. Schuwey, N. Hoyler, A. Gossauer, *J. Org. Chem.* **2001**, *66*, 4973–4988; b) A. Khatyr, R. Ziessel, *J. Org. Chem.* **2000**, *65*, 3126–3134; c) J. S. Moore, *Acc. Chem. Res.* **1997**, *30*, 402–413; d) V. Hensel, A. Godt, R. Popovitz-Biro, H. Cohen, T. R. Jensen, K. Kjaer, I. Weissbuch, E. Lifshitz, M. Lahav, *Chem. Eur. J.* **2002**, *8*, 1413–1423; e) U. H. F. Bunz, *Adv. Polym. Sci.* **2005**, *177*, 1–52; f) P. F. H. Schwab, M. D. Levin, J. Michl, *Chem. Rev.* **1999**, *99*, 1863–1933; g) C. Grave, A. D. Schlüter, *Eur. J. Org. Chem.* **2002**, 3075–3098.
[2] J. Wilhelm, E. Frey, *Phys. Rev. Lett.* **1996**, *77*, 2581–2584.
[3] a) G. Jeschke, A. Koch, U. Jonas, A. Godt, *J. Magn. Reson.* **2002**, *155*, 72–82; b) M. K. Bowman, A. G. Maryasov, N. Kim, V. J. DeRose, *Appl. Magn. Reson.* **2004**, *26*, 23–29; c) G. Jeschke, G. Panek, A. Godt, A. Bender, H. Paulsen, *Appl. Magn. Reson.* **2004**, *26*, 223–244; d) A. D. Milov, Y. D. Tsvetkov, F. Formaggio, S. Oancea, C. Toniolo, J. Raap, *Phys. Chem. Chem. Phys.* **2004**, *6*, 3596–3603; e) W.-Y. Chiang, P. P. Borbat, J. H. Freed, *J. Magn. Reson.* **2005**, *172*, 279–295; f) G. Jeschke, V. Chechik, P. Ionita,

A. Godt, H. Zimmermann, J. Banham, C. R. Timmel, D. Hilger, H. Jung, *Appl. Magn. Reson.* in press.
[4] a) A. D. Milov, K. M. Salikhov, M. D. Shirov, *Fiz. Tverd. Tela* **1981**, *23*, 975 – 982; b) R. E. Martin, M. Pannier, F. Diederich, V. Gramlich, M. Hubrich, H. W. Spiess, *Angew. Chem.* **1998**, *110*, 2994 – 2998; *Angew. Chem. Int. Ed.* **1998**, *37*, 2834 – 2837; c) M. Pannier, S. Veit, A. Godt, G. Jeschke, H. W. Spiess, *J. Magn. Reson.* **2000**, *142*, 331 – 340; d) G. Jeschke, A. Bender, H. Paulsen, H. Zimmermann, A. Godt, *J. Magn. Reson.* **2004**, *169*, 1 – 12.
[5] S. Pornsuwan, G. Bird, C. E. Schafmeister, S. Saxena, *J. Am. Chem. Soc.* **2006**, *128*, 3876 – 3877.
[6] H. Kukula, S. Veit, A. Godt, *Eur. J. Org. Chem.* **1999**, 277 – 286.
[7] a) P. M. Cotts, T. M. Swager, Q. Zhou, *Macromolecules* **1996**, *29*, 7323 – 7328; b) compounds **2**–**5** differ, for synthetic reasons, from polyPPEs by one ethynylene unit. Nevertheless, a comparison of the data seems admissible.
[8] a) Y. Zhou, G. S. Chirikjian, *Macromolecules* **2006**, *39*, 1950 – 1960; b) D. Hu, J. Yu, K. Wong, B. Bagchi, P. J. Rossky, P. F. Barbara, *Nature* **2000**, *405*, 1030 – 1033.
[9] A. Schweiger, G. Jeschke, *Principles of Pulse Electron Paramagnetic Resonance*, Oxford University Press, Oxford, **2001**.
[10] a) D. Hinderberger, O. Schmelz, M. Rehahn, G. Jeschke, *Angew. Chem.* **2004**, *116*, 4716 – 4721; *Angew. Chem. Int. Ed.* **2004**, *43*, 4616 – 4621; b) O. Schiemann, N. Piton, Y. G. Mu, G. Stock, J. W. Engels, T. F. Prisner, *J. Am. Chem. Soc.* **2004**, *126*, 5722 – 5729; c) P. P. Borbat, J. H. Davis, S. E. Butcher, J. H. Freed, *J. Am. Chem. Soc.* **2004**, *126*, 7746 – 7747; d) J. E. Banham, C. R. Timmel, R. J. M. Abbott, S. M. Lea, G. Jeschke, *Angew. Chem.* **2006**, *118*, 1074 – 1077; *Angew. Chem. Int. Ed.* **2006**, *45*, 1058 – 1061.
[11] A. Godt, C. Franzen, S. Veit, V. Enkelmann, M. Pannier, G. Jeschke, *J. Org. Chem.* **2000**, *65*, 7575 – 7582.
[12] a) T. A. Halgren, *J. Comput. Chem.* **1996**, *17*, 490 – 519; b) T. A. Halgren, *J. Comput. Chem.* **1996**, *17*, 520 – 552; c) T. A. Halgren, *J. Comput. Chem.* **1996**, *17*, 553 – 586; d) T. A. Halgren, R. B. Nachbar, *J. Comput. Chem.* **1996**, *17*, 587 – 615; e) T. A. Halgren, *J. Comput. Chem.* **1996**, *17*, 616 – 641.
[13] a) R. G. Larsen, D. J. Singel, *J. Chem. Phys.* **1993**, *98*, 5134 – 5146; b) A. Maryasov, Y. Tsvetkov, J. Raap, *Appl. Magn. Reson.* **1998**, *14*, 101 – 113; c) E. Narr, A. Godt, G. Jeschke, *Angew. Chem.* **2002**, *114*, 4063 – 4066; *Angew. Chem. Int. Ed.* **2002**, *41*, 3907 – 3910.
[14] B. L. Farmer, B. R. Chapman, D. S. Dudis, W. W. Adams, *Polymer* **1993**, *34*, 1588 – 1601.
[15] R. A. Vaia, D. Dudis, J. Henes, *Polymer* **1998**, *39*, 6021 – 6036.
[16] a) U. H. F. Bunz, *Acc. Chem. Res.* **2001**, *34*, 998 – 1010; b) R. Pizzoferrato, M. Berliocchi, A. Carlo, P. Lugli, M. Venanzi, A. Micozzi, A. Ricci, C. Lo Sterzo, *Macromolecules* **2003**, *36*, 2215 – 2223.

